Modeling and measurement of the noise figure of a cascaded non-degenerate phase-sensitive parametric amplifier

Zhi Tong,[1,*] Adonis Bogris,[2] Carl Lundström,[1] C. J. McKinstrie,[3] Michael Vasilyev,[4] Magnus Karlsson,[1] and Peter A. Andrekson[1]

[1]*Photonics Laboratory, Department of Microtechnology and Nanoscience, Chalmers University of Technology, SE-412 96 Göteborg, Sweden*

[2]*Department of Informatics and Telecommunications, National and Kapodistrian University of Athens, 15784 Athens, Greece*

[3]*Bell Laboratories, Alcatel-Lucent, Holmdel, NJ 07733, USA*

[4]*Department of Electrical Engineering, University of Texas at Arlington, 416 Yates St. Arlington, TX 76019-0016, USA*

**zhi.tong@chalmers.se*

Abstract: Semi-classical noise characteristics are derived for the cascade of a non-degenerate phase-insensitive (PI) and a phase-sensitive (PS) fiber optical parametric amplifier (FOPA). The analysis is proved to be consistent with the quantum theory under the large-photon number assumption. Based on this, we show that the noise figure (NF) of the PS-FOPA at the second stage can be obtained via relative-intensity-noise (RIN) subtraction method after averaging the signal and idler NFs. Negative signal and idler NFs are measured, and <2 dB NF at >16 dB PS gain is estimated when considering the combined signal and idler input, which is believed to be the lowest measured NF of a non-degenerate PS amplifier to this date. The limitation of the RIN subtraction method attributed to pump transferred noise and Raman phonon induced noise is also discussed.

OCIS codes: (060.2320) Fiber optics amplifiers and oscillators; (190.4380) Nonlinear optics, four-wave mixing.

References and links

1. C. M. Caves, "Quantum limits on noise in linear amplifiers," Phys. Rev. D Part. Fields **26**(8), 1817–1839 (1982).
2. M. E. Marhic, C. H. Hsia, and J. M. Jeong, "Optical amplification in a nonlinear fibre interferometer," Electron. Lett. **27**(3), 210–211 (1991).
3. K. Croussore, and G. Li, "Phase regeneration of NRZ-DPSK based on symmetric-pump phase-sensitive amplification," IEEE Photon. Technol. Lett. **19**(11), 864–866 (2007).
4. D. Levandovsky, M. Vasilyev, and P. Kumar, "Amplitude squeezing of light by means of a phase-sensitive fiber parametric amplifier," Opt. Lett. **24**(14), 984–986 (1999).
5. D. Levandovsky, M. Vasilyev, and P. Kumar, "Near-noiseless amplification of light by a phase-sensitive fibre amplifier," PRAMANA–, J. Phys. **56**, 281–285 (2001).
6. W. Imajuku, A. Takada, and Y. Yamabayashi, "Low-noise amplification under the 3dB noise figure in high-gain phase-sensitive fibre amplifier," Electron. Lett. **35**(22), 1954–1955 (1999).
7. W. Imajuku, and A. Takada, "Error-free operation of in-line phase-sensitive amplifier," Electron. Lett. **34**(17), 1673–1674 (1998).
8. M. Vasilyev, "Phase-sensitive amplification in optical fibers," in *Frontiers in Optics*, Technical Digest (Optical Society of America, 2005), paper FThB1.
9. R. Tang, P. S. Devgan, V. S. Grigoryan, P. Kumar, and M. Vasilyev, "In-line phase-sensitive amplification of multi-channel CW signals based on frequency nondegenerate four-wave-mixing in fiber," Opt. Express **16**(12), 9046–9053 (2008), http://www.opticsinfobase.org/abstract.cfm?URI=oe-16-12-9046.
10. R. Tang, P. Devgan, V. S. Grigoryan, and P. Kumar, "Inline frequency-non-degenerate phase-sensitive fibre parametric amplifier for fibre-optic communication," Electron. Lett. **41**(19), 1072–1074 (2005).
11. R. Tang, J. Lasri, P. S. Devgan, V. S. Grigoryan, P. Kumar, and M. Vasilyev, "Gain characteristics of a frequency nondegenerate phase-sensitive fiber-optic parametric amplifier with phase self-stabilized input," Opt. Express **13**(26), 10483–10493 (2005), http://www.opticsinfobase.org/oe/abstract.cfm?uri=oe-13-26-10483.
12. P. L. Voss, K. G. Köprülü, and P. Kumar, "Raman-noise-induced quantum limits for $\chi^{(3)}$ nondegenerate phase-sensitive amplification and quadrature squeezing," J. Opt. Soc. Am. B **23**(4), 598–610 (2006).

#126593 - $15.00 USD Received 12 Apr 2010; revised 9 Jun 2010; accepted 16 Jun 2010; published 28 Jun 2010

13. C. J. McKinstrie, S. Radic, and M. G. Raymer, "Quantum noise properties of parametric amplifiers driven by two pump waves," Opt. Express **12**(21), 5037–5066 (2004), http://www.opticsinfobase.org/abstract.cfm?URI=oe-12-21-5037.
14. C. J. McKinstrie, M. Yu, M. G. Raymer, and S. Radic, "Quantum noise properties of parametric processes," Opt. Express **13**(13), 4986–5012 (2005), http://www.opticsinfobase.org/oe/abstract.cfm?uri=OE-13-13-4986.
15. M. Vasilyev, "Distributed phase-sensitive amplification," Opt. Express **13**(19), 7563–7571 (2005), http://www.opticsinfobase.org/oe/abstract.cfm?uri=OE-13-19-7563.
16. C. J. McKinstrie, M. G. Raymer, S. Radic, and M. Vasilyev, "Quantum mechanics of phase-sensitive amplification in a fiber," Opt. Commun. **257**(1), 146–163 (2006).
17. C. Lundström, J. Kakande, P. A. Andrekson, Z. Tong, M. Karlsson, P. Petropoulos, F. Parmigiani, and D. J. Richardson, "Experimental comparison of gain and saturation characteristics of a parametric amplifier in phase-sensitive and phase-insensitive mode," in *European Conference on Optical Communications*, paper Mo. 1.1.1 (2009).
18. J. Kakande, C. Lundström, P. A. Andrekson, Z. Tong, M. Karlsson, P. Petropoulos, F. Parmigiani, and D. J. Richardson, "Detailed characterization of afiber-optic parametric amplifier in phase-sensitive and phase-insensitive operation," Opt. Express **18**(5), 4130–4137 (2010), http://www.opticsinfobase.org/oe/abstract.cfm?URI=oe-18-5-4130.
19. O. K. Lim, V. S. Grigoryan, M. Shin, and P. Kumar, "Ultra-low-noise inline fiber-optic phase-sensitive amplifier for analog optical signals," in *Optical Fiber Communications Conference*, paper OML3 (2008).
20. Z. Tong, C. Lundström, A. Bogris, M. Karlsson, P. Andrekson, and D. Syvridis, "Measurement of sub-1 dB noise figure in a non-degenerate cascaded phase-sensitive fiber parametric amplifier," in *European Conference on Optical Communications*, paper Mo. 1.1.2 (2009).
21. G. Obarski, "Precise calibration for optical amplifier noise figure measurement using the RIN subtraction method," in *Optical Fiber Communications Conference*, paper ThZ3 (2003).
22. E. Desuvire, *Erbium-doped fiber amplifiers* (John Wiley and Sons, 1994), Chap. 2.
23. P. Kylemark, P.-O. Hedekvist, H. Sunnerud, M. Karlsson, and P. A. Andrekson, "Noise characteristics of fiber optical parametric amplifiers," J. Lightwave Technol. **22**(2), 409–416 (2004).
24. A. Mecozzi, and P. Tombesi, "Parametric amplification and signal-to-noise ratio in optical transmission lines," Opt. Commun. **75**(3-4), 256–262 (1990).
25. N. A. Olsson, "Lightwave systems with optical amplifiers," J. Lightwave Technol. **7**(7), 1071–1082 (1989).
26. E. Desuvire, "Comments on 'The noise figure of optical amplifiers'," IEEE Photon. Technol. Lett. **11**(5), 620–621 (1999).
27. Z. Tong, C. J. McKinstrie, C. Lundström, M. Karlsson, and P. A. Andrekson, "Noise performance of optical fiber transmission links that use non-degenerate cascaded phase-sensitive amplifiers," Opt. Express (submitted to).
28. M. Movassaghi, M. K. Jackson, V. M. Smith, and W. J. Hallam, "Noise figure of erbium-doped fiber amplifiers in saturated operation," J. Lightwave Technol. **16**(5), 1461–1465 (1998).
29. P. L. Voss, and P. Kumar, "Raman-effect induced noise limits on $\chi^{(3)}$ parametric amplifiers and wavelength converters," J. Opt. B Quantum Semiclassical Opt. **6**(8), 762–770 (2004) (and references therein).
30. P. Kylemark, P. –O. Hedekvist, H. Sunnerud, M. Karlsson and P. A. Andrekson, "Noise characteristics of fiber optical parametric amplifiers," J. Lightwave Technol. **22**, 409–416 (2004) and **23**, 2192 (2005).
31. Z. Tong, A. Bogris, M. Karlsson, and P. A. Andrekson, "Full characterization of the signal and idler noise figure spectra in single-pumped fiber optical parametric amplifiers," Opt. Express **18**(3), 2884–2893 (2010), http://www.opticsinfobase.org/oe/abstract.cfm?URI=oe-18-3-2884.
32. P. Kylemark, M. Karlsson, and P. A. Andrekson, "Gain and wavelength dependence of the noise-figure in fiber optical parametric amplifiers," IEEE Photon. Technol. Lett. **18**(11), 1255–1257 (2006).
33. X. Li, J. Chen, P. Voss, J. Sharping, and P. Kumar, "All-fiber photon-pair source for quantum communications: Improved generation of correlated photons," Opt. Express **12**(16), 3737–3744 (2004), http://www.opticsinfobase.org/oe/abstract.cfm?URI=oe-12-16-3737.

1. Introduction

One unique advantage of parametric amplifiers is that they can operate in the phase-sensitive (PS) mode, which will lead to the highly attractive noiseless amplification [1]. Two types of PS amplifiers (PSAs) have been investigated so far, which are frequency degenerate (signal and idler frequencies are identical, which can be realized in an interferometer-based [2] or a four-wave-mixing based [3] scheme) and non-degenerate (frequencies are different) cases. The first nearly noiseless fiber PSA was demonstrated by Levandovsky *et. al* [4, 5]. Imajuku *et. al* have measured a 1.8 dB NF (however, at 16 GHz electrical frequency to avoid the guided acoustic-wave Brillouin scattering, or GAWBS) at 16 dB gain in a degenerate PSA [6], and also demonstrated the error-free amplification [7]. However, the inherent single-channel amplification provided by a degenerate PSA, limits dramatically its potential applications. In contrast, non-degenerate PSAs can realize exponential gain [8] and multi-channel amplification [9] without suffering from GAWBS, which makes them more promising in WDM systems. Unfortunately, rigorous phase- and frequency-locking among

#126593 - $15.00 USD Received 12 Apr 2010; revised 9 Jun 2010; accepted 16 Jun 2010; published 28 Jun 2010

the pump, signal and idler are required for a non-degenerate PSA. To date, two different methods based on electrically modulated side-band generation [10] and parametric phase-insensitive amplification [11], respectively, have been proposed to provide the stably-locked input waves. Particularly the latter one, which uses a phase-insensitive amplifier (PIA) as the first stage and then forms a cascaded PIA + PSA scheme, is practically more attractive since the gain band of the former method is severely limited by the electrical modulation bandwidth, and the latter scheme is also compatible with the existing optical systems which use single-carrier signals (no need to use two separate input wavelengths carrying the same information [10]).

Though a lot of theoretical work has been done on both gain and noise properties of a non-degenerate PS-FOPAs [12–16], most previous experimental studies mainly focused on the gain aspects [11,17,18], and only a few of them measured the noise performance. Lim *et. al* [19] (electrical side-band generation) and Tong *et. al* [20] (cascaded PIA+PSA) have measured less than 1 dB signal NFs in non-degenerate PS-FOPAs. However, according to Ref [14,15], an ideal minimum NF in these cases should be −3 dB when only considering the signal or idler wave (due to the constructive interference between the signal and idler fields), which corresponds to the well-known 0 dB 'real' NF accounting for the combined signal and idler. This negative NF is a very interesting and unique characteristic of the frequency non-degenerate PSAs, but no experimental confirmations have been reported until now.

In this paper, we derive the general output noise formula of a cascaded non-degenerate PS-FOPA in Section 2 based on the semi-classical theory, which is consistent with the exact quantum theory under the large-photon-number assumption. According to this theory, in Section 3 we evaluate the RIN subtraction method which is widely used to measure the PIA NF with excess input noise [21], and the results show that, even though RIN subtraction cannot give an accurate NF of either the signal or idler wave alone in a cascaded PS-FOPA, a good estimate can be obtained by taking the average of the signal and idler NFs. Moreover, the limits of the RIN subtraction method are also discussed. In Section 4, negative signal and idler NFs at the PSA stage have been measured after subtracting the PIA excess noise, and a <2 dB 'real' NF (>1 dB lower than the PIA quantum limit) is estimated at >16 dB PSA gain, which is the lowest NF ever measured in a non-degenerate PSA.

2. Noise characteristics of a cascaded non-degenerate PS-FOPA

The general diagram of a cascaded PS-FOPA is shown in Fig. 1. The first PIA stage will generate an almost equalized idler which has a self-stabilized phase relationship with signal and pump waves, and the following PSA stage will provide the PS amplification. Since the output noise level of the PIA stage is monitored, an inter-stage attenuation (ATT) is introduced to account for the passive component like a coupler (where T and T_a represent the main path loss and the bypass loss of the coupler, respectively, as shown in Fig. 1). Moreover, the inter-stage ATT is important for measuring a low PSA NF, which will be discussed below.

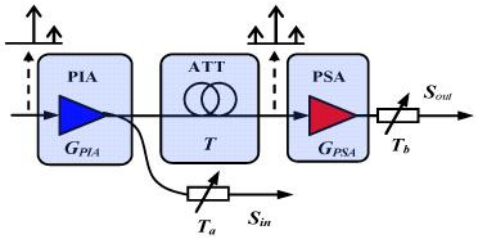

Fig. 1. Schematic of a non-degenerate PIA+ATT+PSA cascade, and the principle diagram of the RIN subtraction measurement. S_{in} and S_{out} are the noise PSD measured at the PSA input and output.

For a conventional PIA+ATT+PIA cascade, the output noise formulas have been discussed in detail in Ref [22]. However, things become more complicated when a cascaded

#126593 - $15.00 USD Received 12 Apr 2010; revised 9 Jun 2010; accepted 16 Jun 2010; published 28 Jun 2010

PS-FOPA with mid-stage ATT is considered, since both correlated (from the parametric amplification) and uncorrelated (from the attenuation) amplitude fluctuations will be produced through the cascade. Quantum theory is usually adopted to obtain the accurate noise characteristics of a PS-FOPA [13,14,16]. Here we carry out a semi-classical analysis to derive the noise performance of a PIA+ATT+PSA cascade, which is consistent with the quantum theory under the high-photon-number assumption, but easier to understand and apply.

As is well known, the general input-output relation of a non-degenerate (two-mode) parametric amplifier in the undepleted pump approximation is given by [13–16]:

$$\begin{bmatrix} A_s \\ A_i^* \end{bmatrix} = \begin{bmatrix} \mu & \nu \\ \nu^* & \mu^* \end{bmatrix} \begin{bmatrix} A_{s0} \\ A_{i0}^* \end{bmatrix} = \mathbf{G} \cdot \begin{bmatrix} A_{s0} \\ A_{i0}^* \end{bmatrix}, \tag{1}$$

where A represents the complex amplitude, subscripts s and i denote signal and idler waves, respectively, A_{s0} is the input signal amplitude, superscript * represents the conjugation operation, μ and ν are the complex transfer coefficients, which depend on both pump and phase-matching conditions, as defined in Ref [15], and also satisfy the auxiliary equation $|\mu|^2 - |\nu|^2 = 1$. Eq. (1) applies to both PI- and PS-FOPAs with single- or dual-pumping. In this paper we only consider the co-polarized pump-signal-idler case to achieve the maximum performance [16]. By including the vacuum fluctuations at the input, we can re-write the input-output relation for the PIA stage as

$$\begin{bmatrix} A_{s,PIA} \\ A_{i,PIA}^* \end{bmatrix} = \begin{bmatrix} \mu_1 & \nu_1 \\ \nu_1^* & \mu_1^* \end{bmatrix} \begin{bmatrix} A_{s0} + \delta A_s \\ \delta A_i^* \end{bmatrix} = \mathbf{G}_1 \cdot \begin{bmatrix} A_{s0} + \delta A_s \\ \delta A_i^* \end{bmatrix}, \tag{2}$$

where δA_s, δA_i denote the uncorrelated vacuum noise fields at signal and idler frequencies. The statistics of the vacuum noise is assumed to be complex Gaussian, and we have $<\delta A_{s,i}>=0$, $<\delta A_{s,i}^2>=0$ and $<|\delta A_{s,i}|^2>=h\nu_{s,i}/2$ [23], where $<\cdot>$ denotes the expectation operation, h is the Planck's constant and ν is the optical frequency. The noise field at $\nu_{s,i}$ can be classically expressed as $|\delta A_{s,i}|\exp[j(2\pi\nu_{s,i}t+\theta)]$ (within 1Hz bandwidth), where θ is the random phase. Subsequently, the attenuation process can be semi-classically modeled as [24]

$$\begin{bmatrix} A_{s,PIA+ATT} \\ A_{i,PIA+ATT}^* \end{bmatrix} = \begin{bmatrix} \sqrt{T_s} & 0 \\ 0 & \sqrt{T_i} \end{bmatrix} \begin{bmatrix} A_{s,PIA} \\ A_{i,PIA}^* \end{bmatrix} + \begin{bmatrix} \sqrt{1-T_s}\delta A_s' \\ \sqrt{1-T_i}\delta A_i' \end{bmatrix} = \hat{\mathbf{T}} \cdot \begin{bmatrix} A_{s,PIA} \\ A_{i,PIA}^* \end{bmatrix}, \tag{3}$$

where $\hat{\mathbf{T}}$ represents the attenuation operator, which behaves like a 4-port beam-splitter coupling the vacuum fields to the signal and the idler, T is the transmittance, and $\delta A_{s,i}'$ represents the newly-introduced uncorrelated vacuum fluctuations through the loss process. For simplicity, we assume that $T_s = T_i = T$. In addition, relative phase shift between the signal and idler will be induced by the dispersion of the attenuator unless perfect dispersion compensation is conducted, which means that the signal and idler fields should be multiplied by the additional phase shifts $e^{j\varphi_1}$ and $e^{j\varphi_2}$, respectively. Similarly from Eq. (1), the input-output relation of the PSA stage is

$$\begin{bmatrix} A_{s,PIA+ATT+PSA} \\ A_{i,PIA+ATT+PSA}^* \end{bmatrix} = \begin{bmatrix} \mu_2 & \nu_2 \\ \nu_2^* & \mu_2^* \end{bmatrix} \begin{bmatrix} e^{j\varphi_1} & 0 \\ 0 & e^{-j\varphi_2} \end{bmatrix} \begin{bmatrix} A_{s,PIA+ATT} \\ A_{i,PIA+ATT}^* \end{bmatrix} = \mathbf{G}_2 \cdot \mathbf{D} \cdot \begin{bmatrix} A_{s,PIA+ATT} \\ A_{i,PIA+ATT}^* \end{bmatrix}, \tag{4}$$

where $\mathbf{D}$ represents the additional phase shift induced by the mid-stage dispersion. By combining Eqs. (2)-(4), we have the output fields of the whole cascade as

#126593 - $15.00 USD Received 12 Apr 2010; revised 9 Jun 2010; accepted 16 Jun 2010; published 28 Jun 2010

$$\begin{bmatrix} A_{s,PIA+ATT+PSA} \\ A_{i,PIA+ATT+PSA}^{*} \end{bmatrix} = \mathbf{G}_2\mathbf{D}\hat{\mathbf{T}}\mathbf{G}_1 \begin{bmatrix} A_{s0}+\delta A_s \\ \delta A_i^{*} \end{bmatrix}$$
$$= \sqrt{T}\begin{bmatrix} \mu_{s12} & \nu_{s12} \\ \nu_{i12}^{*} & \mu_{i12}^{*} \end{bmatrix}\begin{bmatrix} A_{s0}+\delta A_s \\ \delta A_i^{*} \end{bmatrix} + \sqrt{1-T}\begin{bmatrix} \mu_2 e^{j\varphi_1} & \nu_2 e^{-j\varphi_2} \\ \nu_2^{*} e^{j\varphi_1} & \mu_2^{*} e^{-j\varphi_2} \end{bmatrix}\begin{bmatrix} \delta A_s' \\ \delta A_i^{*\prime} \end{bmatrix}, \quad (5)$$
$$= \sqrt{T}\begin{bmatrix} \mu_{s12} & \nu_{s12} \\ \nu_{i12}^{*} & \mu_{i12}^{*} \end{bmatrix}\begin{bmatrix} A_{s0}+\delta A_s \\ \delta A_i^{*} \end{bmatrix} + \sqrt{1-T}\begin{bmatrix} \mu_2 e^{j\varphi_1} & \nu_2 e^{-j\varphi_2} \\ \nu_2^{*} e^{j\varphi_1} & \mu_2^{*} e^{-j\varphi_2} \end{bmatrix}\begin{bmatrix} \delta A_s' \\ \delta A_i^{*\prime} \end{bmatrix},$$

where

$$\mu_{s12} = \mu_1\mu_2 e^{j\varphi_1} + \nu_1^{*}\nu_2 e^{-j\varphi_2}, \nu_{s12} = \nu_1\mu_2 e^{j\varphi_1} + \mu_1^{*}\nu_2 e^{-j\varphi_2},$$
$$\mu_{i12} = \mu_1\mu_2 e^{j\varphi_2} + \nu_1^{*}\nu_2 e^{-j\varphi_1}, \nu_{i12} = \nu_1\mu_2 e^{j\varphi_2} + \mu_1^{*}\nu_2 e^{-j\varphi_1}. \quad (6)$$

The first term at the right side of Eq. (5) denotes the output signal/idler plus the PSA amplified correlated noise components generated from the PIA stage, while the second term represents the PSA amplified uncorrelated noise induced by the mid-stage attenuation. It can be deduced from Eq. (6) that

$$G_{12}(\phi) = |\mu_{s12}|^2 = |\mu_{i12}|^2 = |\mu_1\mu_2|^2 + |\nu_1\nu_2|^2 + 2|\mu_1\mu_2\nu_1\nu_2|\cos(\phi)$$
$$= G_1G_2 + (G_1-1)(G_2-1) + 2\sqrt{G_1G_2(G_1-1)(G_2-1)}\cos(\phi), \quad (7)$$

$$G_{12}(\phi) - 1 = |\nu_{s12}|^2 = |\nu_{i12}|^2 = |\nu_1\mu_2|^2 + |\mu_1\nu_2|^2 + 2|\mu_1\mu_2\nu_1\nu_2|\cos(\phi)$$
$$= (G_1-1)G_2 + G_1(G_2-1) + 2\sqrt{G_1G_2(G_1-1)(G_2-1)}\cos(\phi), \quad (8)$$

where subscripts *1* and *2* denote the PIA and PSA, respectively, G_{12} represents the total signal gain of the PIA + PSA cascade (without ATT), $G_1 = |\mu_1|^2$ is the signal parametric gain of the PIA stage and $G_1 - 1 = |\nu_1|^2$ is the idler conversion efficiency, while $G_2 = |\mu_2|^2$ denotes the PI gain of the PSA stage (when no idler is launched), and similarly we have $G_2 - 1 = |\nu_2|^2$. Thus the PSA gain of the second stage can be expressed as

$$G_{s,PSA}(\phi) = G_{12}(\phi)/G_1, G_{i,PSA}(\phi) = [G_{12}(\phi)-1]/(G_1-1). \quad (9)$$

From Eq. (9) we note that the PS gain depends on the relative phase ϕ, which satisfies the relation $\phi = \phi_{\mu 1} + \phi_{\mu 2} + \phi_{\nu 1} - \phi_{\nu 2} + \varphi_1 + \varphi_2$ ($\phi_{\mu,\nu}$ represent the phase angles of μ and ν, respectively). By optimizing the relative phase among the pump, signal and idler waves (e.g. by choosing the proper inter-stage phase shifts [11], i.e. φ_1 and φ_2, to ensure $\phi = 2m\pi, m = 0, 1, 2, \ldots$), one can obtain the maximum PSA gains for signal and idler as

$$G_{s,PSA}(2m\pi) = (|\mu_1\mu_2| + |\nu_1\nu_2|)^2 / |\mu_1|^2 = [\sqrt{G_1G_2} + \sqrt{(G_1-1)(G_2-1)}]^2 / G_1, \quad (10)$$

$$G_{i,PSA}(2m\pi) = (|\nu_1\mu_2| + |\mu_1\nu_2|)^2 / |\nu_1|^2 = [\sqrt{(G_1-1)G_2} + \sqrt{G_1(G_2-1)}]^2 / (G_1-1). \quad (11)$$

One can easily find that when G_1 and G_2 are much larger than 1,

$$G_{s,PSA}(2m\pi) \approx G_{i,PSA}(2m\pi) \approx 4G_2, \quad (12)$$

which is consistent with the reported 6 dB gain advantage of a non-degenerate PS-FOPA [11,17,18]. In fact, the idler has a slightly larger PS gain than the signal. On the other hand, when $\phi = (2m+1)\pi$ the maximum PS attenuation can also be derived as

#126593 - $15.00 USD Received 12 Apr 2010; revised 9 Jun 2010; accepted 16 Jun 2010; published 28 Jun 2010

$$G_{s,PSA}[(2m+1)\pi]) \approx (G_1+G_2)^2 / 4G_1^2G_2, \quad G_{i,PSA}[(2m+1)\pi] \approx (G_1-G_2)^2 / 4G_1^2G_2, \quad (13)$$

which means that the signal and idler have different maximum attenuations and the gain-attenuation product $G_{PSA}(2m\pi)G_{PSA}[(2m+1)\pi] \neq 1$. This result which deviates from the conclusions in Refs [9, 14, 15]. is due to the un-equalized signal and idler powers input to the PSA. Actually, the maximum PSA attenuation is sensitive to the input power difference.

To achieve the output intensity noise after the square-law detection, we need to obtain both the expectation and variance of the photocurrent $I_{s,i}$, which satisfies $I_{s,i} = R\left|A_{s,i}\right|^2 B_o$, where $R = q / hv$ is the responsivity of an ideal detector (q is the electron charge, and hv is the photon energy) and B_o is the optical bandwidth. According to the NF definition, an ideal photodetector should be assumed, and the imperfect responsivity can be compensated through a calibration process. Based on the semi-classical method used in Ref [25], the single-sided power spectral densities (PSD) of the output noise at the signal and idler frequencies are

$$S_{s,out} = 4R^2P_{s0}TG_{12}(\phi)\frac{hv_s}{2}\{[2G_{12}(\phi)-1]T+(2G_2-1)(1-T)\}, \quad (14)$$

$$S_{i,out} = 4R^2P_{s0}T[G_{12}(\phi)-1]\frac{hv_s}{2}\{[2G_{12}(\phi)-1]T+(2G_2-1)(1-T)\}, \quad (15)$$

where $P_{s0} = |A_{s0}|^2 B_o$ is the input signal power at the PIA stage. In Eqs. (14)-(15) only the signal-noise beat term is considered, which is reasonable since the noise-noise beat term will become negligible provided that the signal (idler) power is much larger than the noise power along the FOPA (which is the case for most practical communication systems, as discussed in Ref [26].). However, the above results are not valid if the PS gain is much lower than 1 (PS attenuation), where the noise-noise beat term will dominate. The first term in the parentheses of Eq. (14) [or Eq. (15)] originates from the correlated noise induced by the first PIA stage, while the second term comes from the uncorrelated noise introduced by the inter-stage attenuator. The physical meaning of Eqs. (14) and (15) is that the correlated noise and the uncorrelated noise will experience different gain [i.e. $(2G_{12}-1)/(2G_1-1)$ for correlated noise vs. $2G_2-1$ for uncorrelated] in the following PSA. Equations (14)-(15) have been verified by using a full quantum theory in the Appendix, under the large-photon-number assumption. In this paper we will mainly focus on the NF of the PSA stage, while a detailed noise analysis of the whole cascade will be discussed in another paper [27].

3. Evaluation of the RIN subtraction method

Contrary to the conventional PIAs and degenerate PSAs, non-degenerate PS-FOPAs are two-mode devices, the 'real' NF of which can only be derived by measuring both the signal and idler fields simultaneously (e.g. through nonlinear mixing) according to Ref [15]. However, this type of measurement is difficult and impractical. The most straightforward way is to measure the signal and idler NFs separately. When assuming the two input waves are identical and shot-noise limited (with uncorrelated vacuum noise), one has [14,15]

$$NF_{s,i} = (2G-1)/G_{PSA}(\phi), \quad (16)$$

where G is the phase-insensitive gain. The maximum PS gain is $G_{PSA}(2m\pi) = (\sqrt{G}+\sqrt{G-1})^2$ under the in-phase condition, where input amplitudes add coherently. Thus, a −3 dB minimum NF can be obtained for either signal or idler wave at high gain regime, which corresponds to a 0 dB 'real' NF of a two-mode-squeezed PSA taking both signal and idler into account. However, if the input signal and idler have different signal-to-noise ratios (SNR), the NF of the better one will be degraded while that of the poorer one will be improved. Thus it is necessary to measure both signal and idler NFs to get the full picture.

#126593 - $15.00 USD Received 12 Apr 2010; revised 9 Jun 2010; accepted 16 Jun 2010; published 28 Jun 2010

To measure the PSA NF in a PIA + PSA cascade, one needs to subtract the excess noise generated from the PIA to meet the shot-noise-limited input criterion [22]. The most widely used technique to measure the NF of a PIA with excess input noise is the RIN subtraction method [21,28], which assumes that the excess noise generated from the first stage will experience the same gain as signal in the following stage. However, it is still not clear whether this method applies to a non-degenerate cascaded PSA. In this section the validity of the RIN subtraction method will be evaluated based on the aforementioned semi-classical theory.

The principle diagram of the RIN subtraction method is shown in Fig. 1, where an inter-stage attenuator is inserted to both account for the coupler and to reduce the excess noise. The signal (or idler) NF of the PSA stage will be [28]

$$\begin{aligned} NF_s &= 1/G_{s,PSA} + P_{s0}TG_1(S_{s,out} - S_{s,in})/(2h\nu_s I_{s,out}^2), \\ NF_i &= 1/G_{i,PSA} + P_{s0}T(G_1 - 1)(S_{i,out} - S_{i,in})/(2h\nu_i I_{i,out}^2), \end{aligned} \tag{17}$$

where subscript *s, i* denote the signal and the idler waves, respectively, P_0 is the input power to the PIA, while $P_{s0}TG_1$ and $P_{s0}T(G_1 - 1)$ denote the input signal and idler powers to the PSA, respectively. I_{out} is the output DC current, S_{out} and S_{in} are the output and input noise PSD (noted in Fig. 1) of the PSA as defined in Eqs. (14)-(15), measured at the same detected power level (where ideal photodetectors are assumed). This implies that

$$T_a = G_{k,PSA}TT_b, \tag{18}$$

where subscript $k = s, i$ denotes either the signal or the idler wave, T_a and T_b are the variable attenuators before the input and the output noise measurement to adjust the signal/idler power, as marked in Fig. 1. One may also show that

$$\begin{aligned} I_{s,out} &= RP_{s0}G_{12}TT_b, \\ I_{i,out} &= RP_{s0}(G_{12} - 1)TT_b. \end{aligned} \tag{19}$$

First let us consider a hypothetical ideal case in a cascaded PS-FOPA, i.e. $G_1 = |\mu_1|^2 = |\nu_1|^2$ in Eq. (2), which means that the signal and idler will have the same gain and noise performance after the PIA stage, thus a perfectly equalized signal and idler pair can be prepared before the PSA, and that the same PSA gain can be obtained for both signal and idler at the PSA stage. In theory this condition might be reached at a specific wavelength with the assistance of Raman effect [29]. Under this assumption, the input and output single-sided noise PSDs can be expressed based on Eqs. (2)-(3) and (14)-(15)

$$S_{k,in} = 4R^2G_1T_aP_{s0} \cdot \frac{h\nu_k}{2}[2G_1T_a + (1 - T_a)], \tag{20}$$

$$S_{k,out} = 4R^2P_{s0}TT_bG_{12}(\phi) \cdot \frac{h\nu_k}{2}\{[2G_{12}(\phi)T + (2G_2 - 1)(1 - T)]T_b + (1 - T_b)\}, \tag{21}$$

where $k = s, i$ denotes either the signal or idler wave. In this ideal condition, both signal and idler have the same output noise expression. By combining Eqs. (17)-(21) and doing some algebra, the PSA NF formula can be expressed as

$$NF_{ideal}(\phi) = [G_{PSA}(\varphi)T + (2G_2 - 1)(1 - T)]/G_{PSA}(\phi), \tag{22}$$

where $G_{PSA} = G_{s,PSA} = G_{i,PSA}$. From Eq. (22) we can find that the excess noise term generated from the PIA stage, i.e. the first term in the parentheses of Eq. (21), has been totally canceled through the RIN subtraction. At the maximum PS gain [$G_{PSA}(2m\pi) \approx 4G_2$], Eq. (22) will be reduced to $NF_{ideal}(2m\pi) \approx (T + 1)/2$ by assuming $G_2 >> 1$, which means that the minimum

#126593 - $15.00 USD Received 12 Apr 2010; revised 9 Jun 2010; accepted 16 Jun 2010; published 28 Jun 2010

PSA NF measured by RIN subtraction depends on the mid-stage loss. The physics behind this effect is that the input noise of the PSA is a mixture of well correlated (result of the first-stage PIA) and completely uncorrelated (result of mid-stage loss) signal-idler noises, as shown in Eqs. (2)-(3). This makes the results measured via RIN subtraction method to deviate from the pure shot-noise-limited-input condition. When T = 1 (no loss), the NF becomes 1 (0 dB) since the signal and idler noise fields are totally correlated, which will lead to an identical PS amplification for both the mean signal (idler) and the noise power at the maximum gain. Whereas when T = 0 (infinite loss), the PSA NF of either signal or idler will be 1/2 (−3 dB), which is exactly the same result from Eq. (16) since a noisy signal light will eventually converge to the coherent state after enough attenuation. Therefore the inter-stage loss has two different functions, which are 1) reducing the excess noise produced by the PIA stage, and 2) introducing uncorrelated vacuum noise resembling to the single-stage PSA case.

However, in practice $|\mu|^2$ and $|\nu|^2$ are not equal in a parametric amplifier, which makes the input signal and idler SNRs to the PSA not perfectly equalized. By using the equation $|\mu|^2 - |\nu|^2 = 1$, the input and output noise PSD at the signal frequency can be obtained as

$$S_{s,in} = 4R^2 G_1 T_a P_{s0} \cdot \frac{h\nu_s}{2}[(2G_1 - 1)T_a + (1 - T_a)], \tag{23}$$

$$S_{s,out} = 4R^2 P_{s0} T T_b G_{12}(\phi) \cdot \frac{h\nu_s}{2}\{[(2G_{12}(\phi)T + 2G_2(1-T) - 1]T_b + (1 - T_b)\}. \tag{24}$$

Substituting Eq. (23)-(24) into (17) and combining (17)-(19), we have the signal PSA NF as

$$NF_s(\phi) = [2G_2 - 2G_2 T + 2G_{s,PSA}(\phi)T - 1] / G_{s,PSA}(\phi). \tag{25}$$

At the maximum PS gain Eq. (25) is reduced to $NF_s(2m\pi) \approx (3T + 1)/2$, when assuming $G_2 >> 1$. In the same way, the idler PSA NF can also be deduced as

$$NF_i(\phi) = [2G_2 - 2G_2 T + 2T - 1] / G_{i,PSA}(\phi), \tag{26}$$

where $G_{i,PSA}(\phi)$ has been defined in Eq. (9). At the maximum PS gain, the minimum idler NF can be expressed as $NF_i(2m\pi) \approx (1 - T)/2$. Apparently in practical conditions, the NFs measured by using RIN subtraction at both signal and idler waves will diverge from the ideal case. The reason for this deviation is that in a real cascaded parametric amplifier, the mean signal (idler) and the excess noise from the first stage will experience different gain at the PSA due to the unbalanced PIA amplification. In fact, the signal will experience a lower gain ($G_{s,PSA}$) than the excess noise [$(2G_{12} - 1)/(2G_1 - 1)$, according to Eq. (14)], whereas the idler will have a larger gain [$(G_{12} - 1)/(G_1 - 1)$, according to Eq. (9)] than the excess noise, which means that the RIN subtraction tends to overestimate the signal NF (by subtracting less noise power) but underestimate the idler NF (by subtracting more noise power), according to the basic formula Eq. (17). However, by using $G_{s,PSA} \approx G_{i,PSA}$ (when both G_1 and the PS gain are much larger than 1), and combining Eq. (25)-(26), we have the equivalent NF of the PSA after taking average of both the signal and idler NFs as

$$NF_{eq} = (NF_s + NF_i)/2 \approx NF_{ideal}, \tag{27}$$

which represents the actual PSA NF with an equalized signal and idler input. Equation (27) implies that the NF measurement error induced by RIN subtraction can be compensated by averaging the separately-measured signal and idler NFs. In Fig. 2, we compare the minimum ideal NF and the equivalent NF measured by RIN subtraction at different T and PSA gain. According to our calculations, the relative error between the NF_{ideal} and NF_{eq} will be

#126593 - $15.00 USD Received 12 Apr 2010; revised 9 Jun 2010; accepted 16 Jun 2010; published 28 Jun 2010

negligible when G_1 > 7 dB. This conclusion also applies to an un-optimized PSA (where $\cos(\phi) \neq 1$) provided that the signal/idler power is high enough to meet the large-photon-number requirement. As a result, though the RIN subtraction method does not apply to non-degenerate cascaded PSAs when considering only signal or idler channel, accurate NF estimation for the equalized-input case can still be obtained by taking the average of signal and idler NFs. The large mid-stage attenuation de-correlates the signal and idler waves and provides a decent approximation of the case where the two inputs are two independent shot-noise limited waves. Thus, a large mid-stage attenuator is required to measure a low PSA NF.

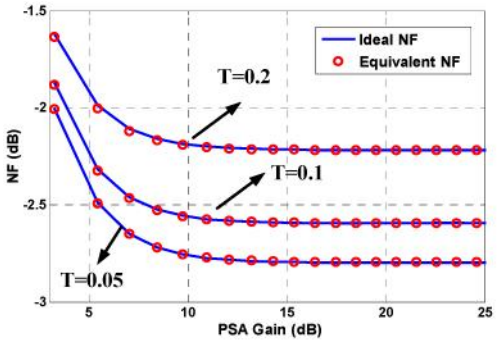

Fig. 2. Comparison of the minimum ideal and equivalent NF vs. PSA gain, according to Eq. (21) and (26), respectively. The PIA gain is fixed at 10 dB.

Until now we only considered the amplified quantum noise (AQN) [30] in the NF analysis, however, other noise contributions [31] such as pump transferred noise (PTN) [32] and Raman induced excess noise [12, 29] will degrade the PIA and PSA noise performance as well. First, we consider the PTN which originates from the ultrafast response of the parametric process. For simplicity we only consider the ideal case where the signal and the idler have identical gains at the PIA. According to Ref [30]. and Eqs. (20)-(21), the excess noise PSDs induced by the PTN at the input and output of the PSA stage are

$$\Delta S_{k,in}^{PTN} = 4[RP_{s0}(\frac{\partial G_1}{\partial P_P})T_a P_P]^2 / (2 \cdot OSNR \cdot \Delta v), \tag{28}$$

$$\Delta S_{k,out}^{PTN} = 4[RP_{s0}(\frac{\partial G_{12}(\phi)}{\partial P_P})TT_b P_P]^2 / (2 \cdot OSNR \cdot \Delta v), \tag{29}$$

where P_P is the launched pump power into the PIA, *OSNR* is the pump optical signal-noise-ratio measured in Δv bandwidth, and factor *2* implies the single-polarization nature of the beat noise, whereas the *OSNR* measurement collects noise from both polarizations. By substituting Eqs. (28)-(29) into (17) and combining (18)-(19), we have

$$\Delta NF_k^{PTN} = \frac{P_{s0}P_P^2 T[(\frac{\partial G_{PSA}}{\partial P_P})^2 G_1 + 2(\frac{\partial G_1}{\partial P_P})(\frac{\partial G_{PSA}}{\partial P_P})G_{PSA}]}{OSNR \cdot G_{PSA}^2 \cdot h\nu_k \Delta v}, \tag{30}$$

where ΔNF_k^{PTN} is the PTN induced additional NF of the PSA stage after RIN subtraction. In Eq. (30), the first term in the numerator describes the exact PTN-induced additional NF of a single-stage PSA (without PIA stage), while the second term is the error term induced by the RIN subtraction, which is due to the nonlinear transfer function of the PTN. As a result, RIN subtraction tends to overestimate the PTN impact on the PSA NF, especially when $\partial G_1 / \partial P_P$ and $\partial G_{PSA} / \partial P_P$ become large (e.g. close to the gain edges).

#126593 - $15.00 USD Received 12 Apr 2010; revised 9 Jun 2010; accepted 16 Jun 2010; published 28 Jun 2010

Next we focus on the Raman induced excess noise, which couples thermal phonons and adds noise to both Stokes and anti-Stokes waves. Raman effect will introduce uncorrelated noise through the fiber [33], while subsequently the parametric process turns those uncorrelated noise photons into correlated photon pairs by generating a conjugated copy at the signal or idler wavelength. This distributed process combining both Raman and four-wave-mixing makes a rigorous noise analysis difficult. Since the correlated noise generated from the PIA will experience the same gain as signal/idler and can be canceled by using RIN subtraction, here we only give a simple and qualitative estimation about the impact of the uncorrelated noise from the first stage on the RIN subtraction method. Considering the hypothetical ideal case ($|\mu_1|^2=|\nu_1|^2$ as used in Eq. (20)) for simplicity and assuming that the Raman effect will induce an uncorrelated optical noise PSD as $F_{k,uc}^{Raman}=rF_{PIA}^{AQN}=2rG_1h\nu_k/2$, at both signal and idler frequencies, where F_{PIA}^{AQN} is the AQN PSD in optical domain at the PIA output, and r is the uncorrelated noise to the output AQN ratio. After the square-law detection, we have

$$\Delta S_{k,in}^{uc}=r\cdot 4R^2G_1^2T_a^2P_{s0}h\nu_k, \tag{31}$$

$$\Delta S_{k,out}^{uc}=r\cdot 4R^2G_{12}^2(\phi)T^2T_b^2P_{s0}(2G_2-1)h\nu_k/G_{PSA}. \tag{32}$$

Combining Eqs. (31)-(32) and (20)-(21), and then substituting them into (17), the impact of uncorrelated PIA noise on the NF measured by RIN subtraction will be

$$\Delta NF_k^{uc}=2rG_1T(2G_2-G_{PSA}-1)/G_{PSA}. \tag{33}$$

Thus, we see that only in the unphysical case where $G_{PSA}=2G_2-1$, there will be no error induced by the uncorrelated noise, otherwise the RIN subtraction method always has inaccurate results. Particularly at the maximum PS gain, the above equation can be reduced to

$$\Delta NF_k^{uc}\approx -rG_1T, \tag{34}$$

which means that the RIN subtraction will underestimate the PSA NF at the optimal gain. This result can be understood by noting that the RIN subtraction will 'subtract' more noise power from the output, since the uncorrelated noise generated at the first stage experiences less gain than signal/idler does at the second stage.

According to Eq. (30) and (33), the accuracy of the RIN subtraction is significantly limited by the PTN and Raman noise generated from the PIA stage. To reduce the measurement inaccuracy, both PTN and Raman noise from the first stage should be kept at a very low level. To achieve low PTN, a very high pump OSNR, a low input signal and a small signal-pump wavelength separation (within ±10 nm) are required [30]. To reduce the Raman induced excess noise, the best way is to move the signal close to the pump wavelength [12, 29]. By carefully designing the cascaded PS-FOPA, the measurement error of the RIN subtraction induced by the PTN and Raman noise will become less important, since the PTN and Raman induced impacts will be partly canceled by each other around the maximum gain. However, the measurement error will drastically increase with the PTN and Raman noise in the PIA. To accurately characterize the noise performance of a non-degenerate PS-FOPA, the best way is to directly launch the shot-noise-limited signal and idler into a phase-locked single-stage PSA, though up to this date it is still challenging to do.

#126593 - $15.00 USD Received 12 Apr 2010; revised 9 Jun 2010; accepted 16 Jun 2010; published 28 Jun 2010

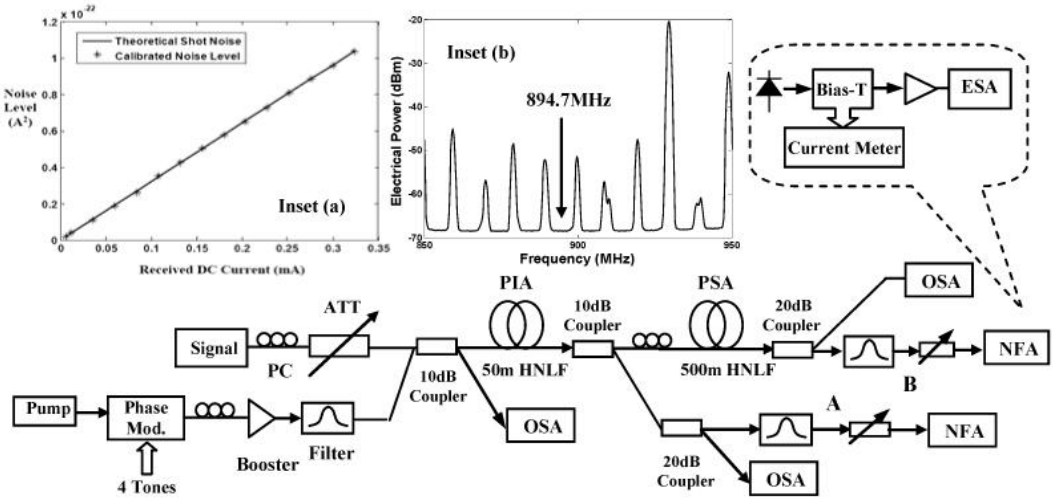

Fig. 3. Measurement setup. NFA: Noise figure analyzer; ESA: Electrical spectrum analyzer; OSA: Optical spectrum analyzer; PC: Polarization controller; ATT: Variable attenuator. Inset (a) shows the theoretical and measured shot noise level after calibration vs. the detected photocurrent, and Inset (b) shows the electrical noise spectrum measured by the ESA, where the spurious tones are due to the pump phase- to intensity-modulation transfer.

4. Experimental results and discussions

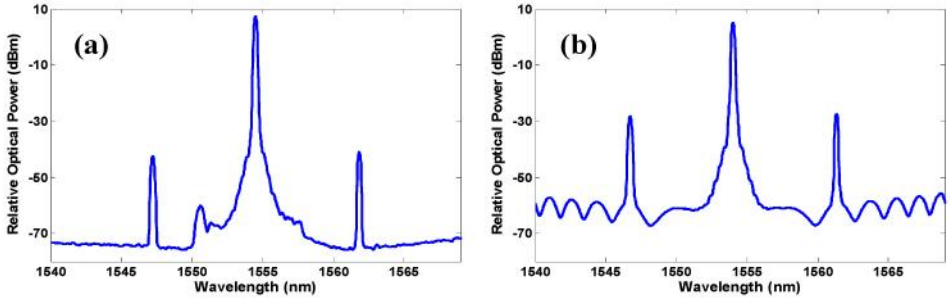

Fig. 4. Measured PSA, PIA gain and PSA NF spectra of the signal wave at a) the anti-Stokes and b) Stokes bands, and the PSA gain and NF spectra of the idler wave at c) the anti-Stokes and d) Stokes bands.

Figure 3 shows the experimental setup. A 60 mW low-noise DFB laser (1554.4 nm) was used as the pump laser, which was phase-modulated by four tones to suppress the stimulated Brillouin scattering (SBS). After an 8.5 W EDFA booster followed by two cascaded 2 nm filters, the amplified pump was combined with the signal by a 10 dB coupler. We use 50 m and 500 m highly nonlinear fibres (HNLF, parameters are λ_0=1552 nm, γ=11.8 $W^{-1}km^{-1}$ and S_0=0.02 ps/nm^2◎km) as the PIA and PSA, respectively. The launched pump power into the PIA and the PSA stages are about 5W and 0.4W, respectively. In between the two stages, another SMF-based 10 dB coupler (SMF length = 7 m) was inserted as the mid-stage attenuator as well as the signal/idler/noise monitor. A polarization controller was also connected with the coupler to align the PIA output waves with the principle axes of the PSA HNLF. We connected the 10% port to the PSA input. A 20 dB coupler was spliced after the PSA to monitor the output spectrum, and two cascaded filters were used to effectively filter out the residual pump and the amplified noise. Finally the amplified signal and idler were detected by the NF analyzer, as shown in Fig. 3.

#126593 - $15.00 USD Received 12 Apr 2010; revised 9 Jun 2010; accepted 16 Jun 2010; published 28 Jun 2010

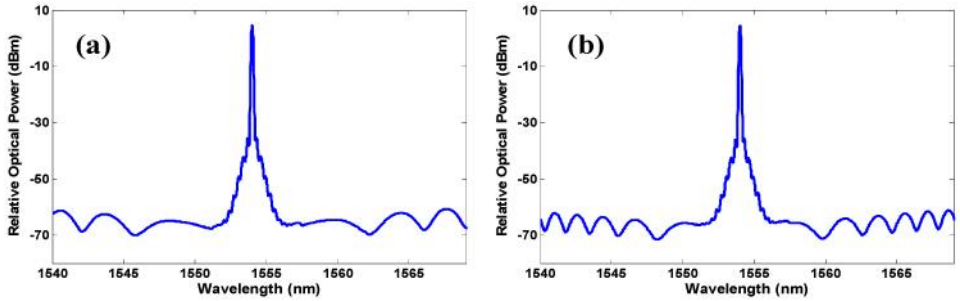

Fig. 5. Output PSA noise spectra with a) 3 m and b) 7 m mid-stage SMF. The OSA resolution bandwidth is 0.1 nm.

The detected signal and noise components were separated by a bias-T, and then measured by a current meter and ESA, respectively. After carrying out calibration for shot noise as shown in inset (a) of Fig. 3, and accurate noise PSD can be measured in the electrical domain. Inset (b) shows the electrical noise spectrum measured by the ESA. We choose 894.7 MHz as the noise measurement frequency to avoid the influence of SBS and reflections. The resolution and the video bandwidths of the ESA are 2 MHz and 3 Hz, respectively, to get a stable noise measurement. After measuring the signal/idler noise powers at the A and B ports, the PSA NF considering signal or idler alone can be estimated by using Eq. (17), while the equivalent NF considering both two waves can be obtained by using Eq. (27). The input and output spectra of the PSA are shown in Fig. 4. In Fig. 4(b), the quasi-periodic peak-dip structure of the output noise spectrum represents the PSA gain changes with the relative phase (induced by the dispersion slope of the mid-stage SMF, as mentioned in Eq. (7)), where the gain peaks imply the optimal PS amplification. As shown in Fig. 5, we can see that a longer mid-stage SMF will make the peak PSA gain closer to the pump wavelength [9], thus the NF measurement at gain peaks will suffer less from both PTN and Raman noise, as mentioned in the last section. Compared with our previous work [20], better pump OSNR (59.4 dB vs. 57 dB), longer PSA HNLF (500 m vs. 250 m) and longer SMF length (7 m vs. 2 m) are adopted here, as a result a better optimal PSA NF can be expected at a larger PSA gain.

#126593 - $15.00 USD Received 12 Apr 2010; revised 9 Jun 2010; accepted 16 Jun 2010; published 28 Jun 2010

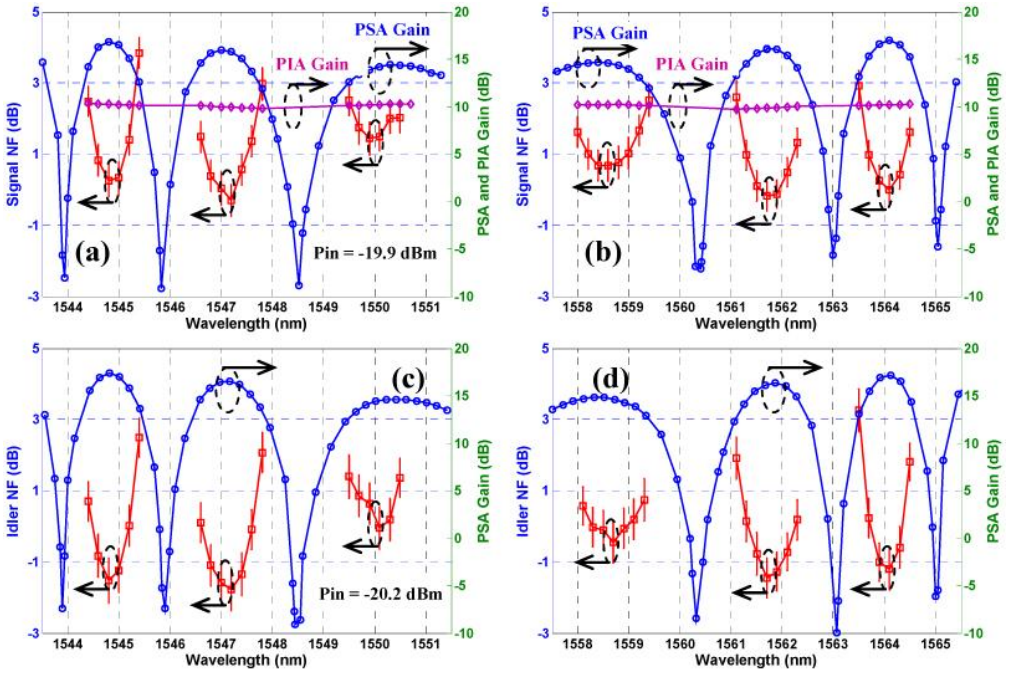

Fig. 6. Measured PSA, PIA gain and PSA NF spectra of the signal wave at a) the anti-Stokes and b) Stokes bands, and the PSA gain and NF spectra of the idler wave at c) the anti-Stokes and d) Stokes bands.

In Figs. 6, the measured PSA gain and NF spectra are shown for the signal and idler waves, respectively, with less than ±0.55 dB measurement error, and the PIA gain spectrum is also shown. The NF measurement error is determined through the differential form of the NF equation [(Eq. (17)]. We can find that the uncertainty of the NF will increase at low output power. In our setup, 10 dB average PIA gain was achieved, which leads to almost balanced (less than 0.5 dB power difference) signal and idler powers input to the PSA, and larger than 16 dB PSA gain can be obtained. To keep both the Raman noise and PTN at low levels, we only measured the NF spectra around the PS gain peaks within ±10 nm pump separation. The input signal and idler powers of the PSA are −19.9 dBm and −20.2 dBm, respectively. According to simulations based on the above parameters, the PTN and Raman induced additional noise increase from the first stage are less than 0.2 dB and 0.6 dB, respectively. The former value will cause a less than 0.5 dB PSA NF overestimation, while the latter one will approximately induce a 0.2-0.4 dB NF underestimation (by assuming that the uncorrelated-to-total Raman noise ratio ranges from 50% to 100%, as a safe estimation), thus the NF measurement error induced by RIN subtraction will be less than 0.3 dB (i.e. NF is slightly overestimated). It should also be mentioned that our measurements provide good estimate of the NF when PS gain is close to its maximum value according to Eq. (27).

From Figs. 6, it is easy to observe an almost symmetrical PSA NF spectrum for both signal and idler at the Stokes and anti-Stokes bands. The slight NF asymmetry observed in Ref [20]. is believed to be due to the measurement uncertainty. Both the signal and idler NFs will increase as the PS gains deviate from the maximum, which agrees well with the theory in [14–16]. Moreover the idler NF is more than 1dB lower than the signal, which is consistent with the results that the RIN subtraction tends to underestimate the idler NF but overestimate the signal NF. We also calculated the averaged NF in Fig. 7, which shows approximately a −1 dB equivalent NF can be estimated at 1547.2 nm and 1561.7 nm. The relatively higher NFs measured at the first two gain lobes are due to the large pump residual noise from the booster. To further look for the optimal PSA NF, in Fig. 8, the signal, idler and equivalent NFs as functions of the input power are shown at 1561.7 nm signal wavelength. The lowest

#126593 - $15.00 USD Received 12 Apr 2010; revised 9 Jun 2010; accepted 16 Jun 2010; published 28 Jun 2010

equivalent NF (signal NF at 1561.7 nm: −0.4 dB, idler NF at 1547.2 nm: −1.7 dB) is measured to be −1 dB in Fig. 8 at about −22 dBm average input. According to Eq. (22), the minimum ideal NF which can be measured by using RIN subtraction is −2.6 dB for T = 0.1 for both signal and idler, which means that the measured minimum equivalent NF is 1.6 dB larger than the ideal value. As a result, a 1.6 dB 'real' PSA NF can be deduced by considering both signal and idler inputs, which is approximately 1.4 dB below the PIA quantum limit. The 1.6 dB NF increase is mainly due to the PTN and Raman induced excess noise, and the former can be clearly seen from the NF increase with the input signal/idler power, as shown in Fig. 8. The impact of polarization mis-alignment on the PSA noise performance is negligible in our setup.

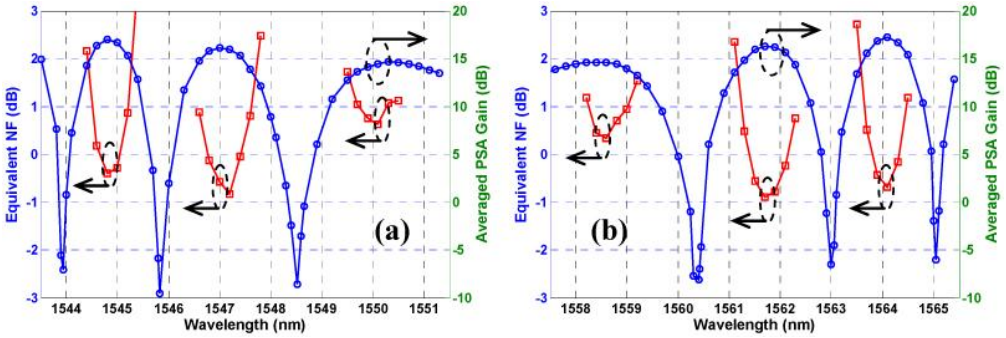

Fig. 7. Averaged PSA gain and equivalent NF spectra by taking average of the signal and idler gains and NFs [Eq. (27)] at a) the anti-Stokes and b) the Stokes bands.

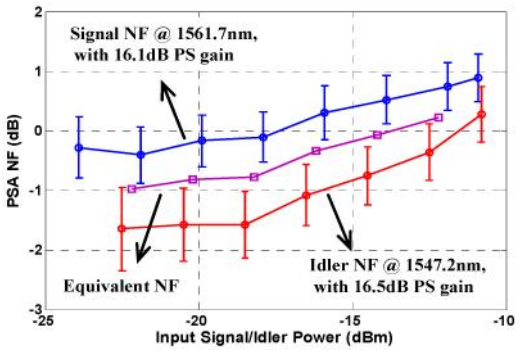

Fig. 8. Measured signal and idler NF as a function of input power, and the estimated equivalent NF at averaged input power. Minimum −1dB equivalent NF can be observed.

5. Conclusions

Based on the semi-classical theory, we derived detailed formulas to characterize the noise performance of a PIA+ATT+PSA cascade, which show that correlated (from the parametric amplification) and uncorrelated (from the loss process) noises between the signal and idler waves experience different gains in the PSA. Based on these results, the validity of the RIN subtraction method is evaluated for a non-degenerate cascaded PS-FOPA. Though this method tends to overestimate the signal NF while underestimate the idler NF, we show that the equivalent NF obtained by taking average of the signal and idler NFs will give a good estimation of the PSA NF. In addition, the accuracy of the RIN subtraction is limited by the PTN and Raman noise generated from the PIA stage. By improving our previous experimental setup, negative NF was measured at both the signal and idler waves, for the first time, to our knowledge. A less than 2 dB 'real' NF was measured by considering the signal

#126593 - $15.00 USD Received 12 Apr 2010; revised 9 Jun 2010; accepted 16 Jun 2010; published 28 Jun 2010

and idler simultaneously, which is the lowest NF ever measured for a non-degenerate PSA. This cascaded scheme is compatible with the existing systems using single-carrier signals.

Appendix: Quantum mechanical derivation of the noise of a PIA+ATT+PSA cascade

Two-mode parametric amplification is governed by the input-output (IO) relations [14]

$$b_s = \mu a_s + \nu a_i^\dagger, \tag{35}$$

$$b_i = \mu a_i + \nu a_s^\dagger, \tag{36}$$

where *a* and *b* are the operators at input and output, *s* and *i* represent the signal- and idler-mode, respectively, and † denotes a Hermitian conjugate. The transfer functions μ and ν satisfy the auxiliary equation $|\mu|^2 - |\nu|^2 = 1$, which ensures that the transformation is canonical. Attenuation is modeled as two-mode beam-splitting, which is governed by

$$b_s = \tau a_s + \rho a_l, \tag{37}$$

$$b_l = -\rho^* a_s + \tau^* a_l, \tag{38}$$

where *s* and *l* represent the signal- and loss-mode, respectively. The transfer functions τ and ρ satisfy the auxiliary equation $|\tau|^2 + |\rho|^2 = 1$. For direct detection, the relevant quantities are the means (photocurrent) and variances (noise power) of the photon numbers. By defining the number and variance operators $n_j = a_j^\dagger a_j$ and $\delta n_j^2 = n_j^2 - \langle n_j \rangle^2$, respectively, the noise characteristics can be determined through the IO relations.

First we consider a PIA followed by parallel ATTs (for both signal and idler modes). The IO relations can be obtained according to Eqs. (35)-(38) as

$$c_s = (\tau_s \mu_1) a_s + (\tau_s \nu_1) a_i^\dagger + \rho_s a_l, \tag{39}$$

$$c_i = (\tau_i \mu_1) a_i + (\tau_i \nu_1) a_s^\dagger + \rho_i a_m, \tag{40}$$

where *c* denotes the output mode, μ_1 and ν_1 are the transfer coefficients for the PIA stage, τ and ρ are the transfer coefficients for the following ATTs, and the subscripts *s, i, l, m* denote signal, idler and two loss modes, respectively. Here we assume that the attenuations for the signal and idler modes are identical, which means that $\tau_s = \tau_i = \tau$ and $\rho_s = \rho_i = \rho$. For PI operation, the input signal mode can be assumed to be a coherent state, for which $\langle \delta n_s^2 \rangle = \langle n_s \rangle$, while the idler input is a vacuum state. Equations (39) and (40) have the same forms as the IO relations considered in [13, 14], so the general formulas derived therein apply to PIA followed by an ATT. The output variances of the signal and idler modes are

$$\langle \delta n_{s\_PIA+ATT}^2 \rangle = |\tau\mu_1|^4 \langle n_s \rangle + |\tau\mu_1|^2 (|\tau\nu_1|^2 + |\rho|^2)\langle n_s \rangle + |\tau\nu_1|^2 (|\tau\mu_1|^2 + |\rho|^2), \tag{41}$$

$$\langle \delta n_{i\_PIA+ATT}^2 \rangle = |\tau\nu_1|^4 \langle n_s \rangle + |\tau\nu_1|^2 (|\tau\mu_1|^2 + |\rho|^2)\langle n_s \rangle + |\tau\nu_1|^2 (|\tau\mu_1|^2 + |\rho|^2), \tag{42}$$

where the first two terms on the right sides of Eq. (41) and (42) represent the signal-noise beat terms, whereas the third terms are the noise-noise beat terms. In practice, the noise-noise terms can be neglected when $\langle n_s \rangle >> 1$ (large-photon-number assumption). Therefore by defining $|\tau|^2 = T$, $|\rho|^2 = 1 - T$, $|\mu_1|^2 = G_1$, $|\nu_1|^2 = G_1 - 1$, and $P_{s0} = \langle n_s \rangle h\nu B_o$, we find that Eq. (41) can be expressed in exactly the same form as Eq. (23) except for the factor $2R^2(h\nu)^2 B_o$. This factor comes from the photon detection and the vacuum fluctuations. Considering the well-known semi-classical shot-noise expression

#126593 - $15.00 USD Received 12 Apr 2010; revised 9 Jun 2010; accepted 16 Jun 2010; published 28 Jun 2010

$\left\langle \Delta I_{shot}^2 \right\rangle = 2qI_s B_e = 4R^2 \left\langle n_s \right\rangle (h\nu)^2 B_o B_e / 2$ (single-sided PSD), where q is the electron charge and $I_s = R\left\langle n_s \right\rangle h\nu B_o$ is the detected photocurrent, we can see this factor is necessary to relate the semi-classical to the quantum results ($\left\langle \delta n_s^2 \right\rangle = \left\langle n_s \right\rangle$). Thus Eq. (23) can be verified by Eq. (41) in a quantum way under the large-photon-number condition. Similarly, the output idler noise formula of the PIA + ATT cascade can also be confirmed by Eq. (42).

Next we consider the more-complicated cascaded PIA + ATT + PSA case. By including the additional phase shifts induced by the mid-stage ATT ($e^{j\phi_1}$ and $e^{j\phi_2}$ for the signal and idler modes, respectively), we have the IO relations in the canonical forms

$$d_s = \mu_{11} a_s + \nu_{12} a_i^\dagger + \mu_{13} a_l + \nu_{14} a_m^\dagger, \tag{43}$$

$$d_i = \nu_{21} a_s^\dagger + \mu_{22} a_i + \nu_{23} a_l^\dagger + \mu_{24} a_m. \tag{44}$$

The composite transfer coefficients are

$$\begin{gathered} \mu_{11} = \mu_2 \mu_1 \tau e^{j\varphi_1} + \nu_2 \nu_1^* \tau^* e^{-j\varphi_2}, \mu_{22} = \mu_2 \mu_1 \tau e^{j\varphi_2} + \nu_2 \nu_1^* \tau^* e^{-j\varphi_1}, \\ \nu_{12} = \mu_2 \nu_1 \tau e^{j\varphi_1} + \nu_2 \mu_1^* \tau^* e^{-j\varphi_2}, \nu_{21} = \mu_2 \nu_1 \tau e^{j\varphi_2} + \nu_2 \mu_1^* \tau^* e^{-j\varphi_1}, \\ \mu_{13} = \mu_{24} = \mu_2 \rho, \nu_{14} = \nu_{23} = \nu_2 \rho^*, \end{gathered} \tag{45}$$

where μ_2 and ν_2 are the transfer coefficients for the PSA stage. It is easy to verify that $|\mu_{11}|^2 - |\nu_{12}|^2 + |\mu_{13}|^2 - |\nu_{14}|^2 = 1$, which ensures that the composite transformation is canonical. Finally by using the aforementioned definitions and the results of [13, 14], one can write the output variances of the signal and idler modes as

$$\begin{aligned} \left\langle \delta n_{s\_PIA+ATT+PSA}^2 \right\rangle = |\mu_{11}|^4 \left\langle n_s \right\rangle + |\mu_{11}|^2 (|\nu_{12}|^2 + |\mu_{13}|^2 + |\nu_{14}|^2) \left\langle n_s \right\rangle \\ + (|\mu_{11}|^2 + |\mu_{13}|^2)(|\nu_{12}|^2 + |\nu_{14}|^2), \end{aligned} \tag{46}$$

$$\begin{aligned} \left\langle \delta n_{i\_PIA+ATT+PSA}^2 \right\rangle = |\nu_{21}|^4 \left\langle n_s \right\rangle + |\nu_{21}|^2 (|\mu_{22}|^2 + |\nu_{23}|^2 + |\mu_{24}|^2) \left\langle n_s \right\rangle \\ + (|\mu_{22}|^2 + |\mu_{24}|^2)(|\nu_{21}|^2 + |\nu_{23}|^2), \end{aligned} \tag{47}$$

where the first two terms on the right sides of Eq. (46) and (47) represent the signal-noise beat terms, while the third terms are the noise-noise beat terms. After neglecting the noise-noise terms under the large-photon-number assumption, and by defining $|\mu_{11}|^2 = G_{12} T$, $|\nu_{12}|^2 = (G_{12} - 1)T$, $|\mu_{13}|^2 = G_2(1-T)$ and $|\nu_{14}|^2 = (G_2 - 1)(1-T)$, we can find that Eq. (46) and (47) are in exactly the same form as Eq. (14) and (15) after multiplying the $2R^2 (h\nu)^2 B_o$ factor, which clearly proves the validity of the semi-classical method.

Acknowledgement

This research leading to these results has received funding from the European Communities 7th Framework Programme FP/2007-2013 under grant agreement 224547 (STREP PHASORS), and also from the Air Force Office of Scientific Research, Air Force Material Command, USAF, under grant number FA8655-09-1-3076. Z. Tong would like to thank Per-Olof Hedekvist for help with error analysis.

#126593 - $15.00 USD Received 12 Apr 2010; revised 9 Jun 2010; accepted 16 Jun 2010; published 28 Jun 2010